On evaluating the hypothesis of shape similarity between soil particle-size distribution and water retention function

Ugo Lazzaro, Caterina Mazzitelli, Benedetto Sica, Paola Di Fiore, Nunzio Romano, Paolo Nasta

Department of Agricultural Sciences, Division of Agricultural, Forest and Biosystems Engineering, University of Naples Federico II, Napoli, Italy

Abstract

Two pedotransfer functions (PTFs) are available in the literature enabling the soil water retention function (WRF) to be estimated from knowledge of the soil particle-size distribution (PSD), oven-dry soil bulk density (ρ_b), and saturated soil water content (θ_s): *i*) the Arya and Heitman model (PTF-AH), and *ii*) the Mohammadi and Vanclooster model (PTF-MV). These physico-empirical PTFs rely on the hypothesis of shape similarity between PSD and WRF, and do not require the calibration of the input parameters. In the first stage, twenty-seven PSD models were evaluated using 4,128 soil samples collected in Campania (southern Italy). These models were ranked according to the root mean square residuals (RMSR), corrected Akaike information criterion (AICc), and adjusted coefficient of determination (R^2_{adj}). In the second stage, three subsets of PSD and WRF data (DS-1, DS-2, and DS-3), comprising 282 soil samples, were used to evaluate the two PTFs using the best three PSD models selected in the first stage. The hypothesis of shape similarity was assumed as acceptable only when the RMSR value was lower than the field standard deviation of the WRFs (σ^*), which is viewed as a tolerance threshold and computed from the physically based scaling approach proposed by Kosugi and Hopmans (1998). In the first study area (DS-1), characterized by a fairly uniform, loamy textured volcanic soil, the PTF-AH outperformed the PTF-MV and both PTFs provided reasonable performance within the acceptance threshold (*i.e.*, RMSR < σ^*). In the other two heterogeneous field sites (DS-2 and DS-3, characterized by soil textural classes that span from clay and clay-loam to loam and even sandy-loam soils), the PTF-MV (with 3% to 6% RMSR surpassing σ^*) outperformed the PTF-AH (with 8% to 30% RMSR surpassing σ^*) and the majority of RMSR values were larger than those obtained in the original studies. The mean relative error (MRE) revealed that the PTF-MV systematically underestimates the measured WRFs, whereas the PTF-AH provided negative MRE values indicating an overall overestimation. The outcomes of our study provide a critical evaluation when using calibration-free PTFs to predict WRFs over large areas.

Correspondence: Paolo Nasta, Department of Agricultural Sciences, Division of Agricultural, Forest and Biosystems Engineering, University of Naples Federico II, Napoli, Italy.
Tel.: +39.0812539012.
E-mail: paolo.nasta@unina.it

Key words: pedotransfer function (PTF); hydrometer; sieving; soil water retention function (WRF); USDA texture classification.

Conflict of interest: the authors declare no potential conflict of interest.

Contributions: the authors contributed equally.

Received: 21 April 2023.
Accepted: 3 August 2023.
Early view: 25 October 2023.

©*Copyright: the Author(s), 2023*
Licensee PAGEPress, Italy
Journal of Agricultural Engineering 2023; LIV:1542
doi:10.4081/jae.2023.1542

This work is licensed under a Creative Commons Attribution-NonCommercial 4.0 International License (CC BY-NC 4.0).

Publisher's note: all claims expressed in this article are solely those of the authors and do not necessarily represent those of their affiliated organizations, or those of the publisher, the editors and the reviewers. Any product that may be evaluated in this article or claim that may be made by its manufacturer is not guaranteed or endorsed by the publisher.

Introduction

The soil water retention function (WRF) is a fundamental soil hydraulic property for modeling hydrologic balance. Large-scale water resources management commonly relies on simplified Richards-equation-based distributed hydrological models which require a massive number of WRFs to be measured through labor-intensive sampling campaigns and time-consuming and tedious laboratory experiments. Alternatively, one can resort to pedotransfer functions (PTFs) that relate the soil hydraulic properties (estimands) to more easily measurable soil physico-chemical attributes (predictors), such as sand, silt, and clay contents, soil organic carbon content, and oven-dry soil bulk density (Van Looy *et al.*, 2017). Empirical PTFs are data-driven models which estimate WRFs from routinely available taxonomic data by using multiple regression equations or machine-learning approaches, such as artificial neural networks, support vector machines, and random forest techniques (Nasta *et al.*, 2021). The empirical PTFs necessitate site-specific calibration procedures because their applicability is often unsuccessful outside the training data domain. By contrast, the so-called physico-empirical PTFs conceptualize the pore space as a bundle of cylindrical capillaries generated by the natural packing of soil particles and postulate the assumption of shape similarity between the particle-size and pore-size distributions (Arya and Paris, 1981; Haverkamp and Parlange, 1986; Nimmo *et al.*, 2007; Mohammadi and Meskini-Vishkaee, 2013; Lee and Ro, 2014; Antinoro *et al.*, 2014; Campos-Guereta *et al.* 2021; You *et al.*, 2022). Moreover, the particle-size distribution (PSD) data can be fitted by using well-established mathematical models based on different numbers of parameters (Hwang *et al.*, 2002; Hwang, 2004; Bah *et al.*, 2009; Bayat *et al.*, 2015; Esmaeelad *et al.*, 2016; Meskini-Vishkaee and Davatgar 2018; Vaz *et al.*, 2020;

Non-commercial use only

Cheshmberah *et al.*, 2022). Bayat *et al.* (2017) evaluated thirty-six PSD models by using 160 soil data and recommended applying such mathematical models on larger data sets.

Recently, two PTFs have emerged in the scientific literature for their independence from database-related empirical parameters: i) the Arya and Heitman model (AH) (Arya and Heitman, 2015); ii) the Mohammadi and Vanclooster model (MV) (Mohammadi and Vanclooster, 2011). Both PTFs require PSD, oven-dry bulk density, and saturated soil water content as input data. Nevertheless, these two PTFs were evaluated on 41 or 80 soil samples, respectively, belonging to the UNSODA database in the original studies (Mohammadi and Vanclooster, 2011; Arya and Heitman, 2015).

The main aim of this study is to evaluate the effectiveness and reliability of the assumption of shape similarity between the PSD and WRF. Based on a large database of soil properties available at the Laboratory of Soil Hydrology of the University of Naples Federico II, this task was carried out in two separate stages: i) in the first stage, we evaluated the performance of twenty-seven PSD models to fit the soil particle-size distributions measured on 4,128 soil samples over the entire region of Campania and identified the best three ones; ii) in the second stage, we used the best PSD models to test the hypothesis of shape similarity between PSD and WRF by applying the PTF-AH and PTF-MV to 282 soil samples gathered from three different experimental areas.

Materials and Methods

Available data and techniques to measure particle-size distribution and water retention function

To test the fitting capability of twenty-seven PSD models we used a total of 4,128 disturbed soil samples collected during different soil survey campaigns in Campania (Nasta *et al.*, 2009; Romano *et al.*, 2018; Palladino *et al.*, 2022). Campania is an administrative region in southern Italy that covers 13,671 km^2 with very diverse morphological, hydrogeological, and pedological features (for details, see the paper by Allocca *et al.*, 2023).

To evaluate the performance of PTF-AH and PTF-MV, we selected 282 soil samples, with the availability of both measured PSD and WRF, gathered in three experimental areas: i) DS-1 comprises 89 disturbed and undisturbed soil samples collected at the soil depth of 40 cm over a 132-m-long transect in a peach orchard located near the city of Acerra (Campania, province of Naples) (Ciollaro and Romano, 1995); ii) DS-2 comprises 105 disturbed and undisturbed soil samples taken from the uppermost soil horizons at locations spaced 50 m apart, along six different transects in the Upper Alento River catchment (Campania, province of Salerno) (Nasta *et al.*, 2009); iii) DS-3 comprises 88 disturbed and undisturbed soil samples collected at the soil depth of 20 cm along two transects in the Fiumarella di Corleto creek catchment (Basilicata, province of Potenza) (Nasta *et al.*, 2009).

Given the purpose of the present study, the PSD measurement merits a larger description and, for all disturbed soil samples, was carried out by starting with a preliminary treatment of each disturbed soil sample to enhance the separation and dispersion of soil aggregates. The dispersing solution was prepared by adding 35.7 g of sodium polyphosphate, $NaPO_3$, and 7.94 g of sodium carbonate, Na_2CO_3 into 1000 mL of deionized water. The disturbed soil samples collected in the field were ground and oven-dried at 40°C for 24 hours. We stirred 40.0 g of soil with 100 mL of dispersing solution with a blade electric mixer in a cup for 5 minutes then transferred this soil solution into a 1000-mL glass cylinder and adjusted the volume to 1000 mL by adding distilled water. We mixed the content thoroughly by using a plunger and added a drop of amyl alcohol if the surface of the suspension was covered by foam. The sedimentation method was conducted by using a standard hydrometer (ASTM 152H with Bouyoucos scale from 0 g L^{-1} to 50 g L^{-1} corresponding to hydrometer lengths of 10.5 cm and 2.3 cm, respectively). After the homogenization of the suspension, the settling velocity depends on the particle diameter. The Stokes law relates the time of settling to the particle size remaining suspended in the solution (Stokes, 1850; Gee and Bauder, 1986). Six manual hydrometer settling depth readings were taken at predefined times of 3, 10, 30, 100, 210, and 1440 minutes by measuring the buoyancy of a floating body with the hydrometer method (Bouyoucos, 1927). Temperature and standard readings in the blank (no soil) solution were recorded at each time step. At the end of the sedimentation method, the sediment and suspension were transferred through a 0.05-mm-diameter square mesh woven bronze wire cloth and oven-dried at 105°C for 24 hours. The resulting dry soil sample was poured onto a nest of sieves with diameters of 1.00 mm, 0.50 mm, 0.25 mm, 0.10 mm, and 0.05 mm. Cumulative sand fractions were weighted to obtain five PSD data (Gee and Or, 2000). A total of eleven PSD data pairs, *i.e.*, particle diameter, d (mm), with corresponding unitless particle mass fraction, P(d) were obtained for each soil sample (Figure 1). We refer to the United States Department of Agriculture (USDA) texture classification to separate sand, silt, and clay contents (primary particle diameters <0.002 mm, 0.002-0.05 mm, 0.05-2.0 mm). Sand fractions were calculated by following Gee and Or (2000), whereas silt fractions were obtained as the complement to 100% (Figure 1). The largest number of soil samples belong to the loam class (N_{loam}=1,079), whereas silt and sandy-clay classes are the least represented.

Before starting any laboratory hydraulic test, each undisturbed soil core was saturated from below according to the protocol developed in our laboratory and described in Romano *et al.* (2002). At the completion of the full saturation step, the saturated soil water content, θ_s, was measured. The volumetric soil water content, θ, was measured using the thermo-gravimetric method. For each soil core belonging to the DS-1 group (Acerra dataset), the soil water retention function was measured by using the evaporation method (Romano and Santini, 1999; Romano and Nasta, 2016). The undisturbed soil core was contained in a steel cylinder (height of 12 cm and inner diameter of 8.6 cm) and initially fully saturated. Three mini-tensiometers were horizontally inserted at different soil depths (2.5 cm, 6.0 cm, and 9.5 cm). After tensiometer calibration, the soil core was placed on a strain-gauge load cell, which monitored the total soil weight, while each mini-tensiometer measured the soil matric pressure head values during the evaporation process. The evaporation rate was accelerated by turning a fan on to blow air on the soil surface. The evaporation test ended when the matric pressure head of the uppermost mini-tensiometer got too low for its proper functioning (up to a matric pressure head of about -600 cm).

The soil water retention data points of the soil cores belonging to the DS-2 (Alento dataset) and DS-3 (Fiumarella dataset) groups were measured by using the suction tables apparatus (Romano *et al.*, 2002). The soil core was collected using steel cylinders (height of 7.05 cm and inner diameter of 7.2 cm). The soil water retention characteristic was determined from saturation to a minimum matric pressure head (h, in cm) of about -400 cm. At the Laboratory of Soil Hydrology, the suction table apparatus consisted of three Perspex containers (with length, width, and height of 57.5 cm, 46.5 cm, 20.0 cm, respectively), each of which can hold

up to twenty-four soil cores. The porous barrier packed at the bottom of each container consisted of one layer of fine material (*i.e.*, kaolin clay). Each container was covered with a lid on top to prevent evaporation. A channel system at the base of the Perspex container allowed for easy water drainage and the removal of air trapped in the channels, which run parallel to the length of the container. The hanging-water column system was used to regulate prescribed suction values up to -100 cm by sliding a constant-level bottle with an overflow tube along a rod. The constant-head Mariotte cylinder system (or bubble towers) set the prescribed *h*-values from -100 cm up to -400 cm. For additional details on the suction tables apparatus, the reader is directed to the chapter by Romano *et al*. (2002). At the end of the laboratory hydraulic tests described above, each soil core was placed in a ventilated oven, at the standard temperature of 105°C and for not less than 24 hours, to measure the oven-dry soil bulk density, ρ_b (g cm^{-3}).

The pressure plate apparatus was used to add three data pairs of the water retention curve in both methods. Disturbed samples were repacked into 5-cm-tall brass rings and placed on porous ceramic plates (Bittelli and Flury, 2009). The θ-values were determined at three prescribed pressure steps between 3,000 cm 15,000 cm. Figure 1 shows the experimental data of the measured WRF in the three data sets and their distribution in the USDA texture triangle. Soil organic carbon (OC) content integrated the above-mentioned datasets and was measured from the sieved soil sample (fine fraction less than 2.0 mm) using the wet combustion method suggested by Mebius (1960) (potassium dichromate method). OC was expressed as % by mass and, by convention, we set the soil organic matter (OM) content equal to OM=1.724×OC (Russel and Engle, 1928).

Particle-size distribution models and performance evaluation

In this study, we evaluated twenty-seven PSD models (reported in Table 1; Rosin and Rammler, 1933; Schuhmann, 1940; Jaky, 1944; Harris, 1968; Mandelbrot, 1983; Buchan, 1989; Kolev *et al.*, 1996; Nemes *et al.*, 1999; Pasikitan, 1999; Zobeck *et al.*, 1999; Bird *et al.*, 2000; Zhuang *et al.*, 2001; Perrier and Bird, 2002; Nesbitt and Breytenbach, 2006), the majority of which were already documented in Bayat *et al.* (2017).

The twenty-seven PSD models were fitted to the eleven measured PSD data pairs by using the least squares curve fitting toolbox of the MATLAB R2019b software (The MathWorks. Inc, Natick, Massachusetts, United States). Reference is made here to the cumulative particle mass fraction of soil particles spanning from 0 (minimum frequency) to 1 (maximum frequency).

The evaluation of PSD model predictive performances was based on the root mean square residual (RMSR), corrected Akaike information criterion (AICc), and adjusted coefficient of determination (R^2_{adj}), defined as follows:

$$RMSR = \sqrt{\frac{1}{n}\sum_{i=1}^{n}(O_i - P_i)^2} \quad (1)$$

$$R^2_{adj} = 1 - \left(1 - \frac{\sum_{i=1}^{n}(O_i - P_i)^2}{\sum_{i=1}^{n}(O_i - \bar{O})^2}\right) \times \frac{(n-1)}{(n-p)} \quad (2)$$

$$AICc = \left[n \times ln\left(\frac{SSE}{n}\right) + n + 2p\right] + \frac{2p(p+1)}{(n-p-1)} \quad (3)$$

where O, $\bar{O}$, and P refer to the observed, the mean of observed, and the predicted values of PSD at particle size i, p is the number of predictors, and n is the total number of PSD data (n=11). In Eq. (3), SSE is the sum of squared errors, given by:

$$SSE = \sum_{i=1}^{n}(O_i - P_i)^2 \quad (4)$$

The optimal prediction is associated with a RMSR value of 0 and a R^2_{adj} value of 1, with the latter metric penalized by the number of model parameters. The AICc (Ayoubi and Karami, 2019) quantifies the trade-off between the goodness of fit and model parsimony and penalizes those redundant models that employ too many parameters with a risk of multicollinearity.

The PTF-AH and PTF-MV performance evaluation

The measured water retention data pairs (h-θ) of soil matric pressure head, h (cm), and volumetric water content, θ (cm^3 cm^{-3}), were fitted to Kosugi's analytical expression (Kosugi, 1996) which relates the degree of saturation, S_e, to the natural logarithm of h (ln$h$) as follows:

$$S_e(lnh) = \frac{\theta - \theta_r}{\theta_s - \theta_r} = \frac{1}{2} erf\left(\frac{lnh - \ln h_m}{\sigma\sqrt{2}}\right) \quad (5)$$

where lnh_m and σ are the mean and standard deviation of ln$h$, θ_r (cm^3 cm^{-3}) is the residual soil water content. For convenience θ_r was assumed as zero so that only the two unknown parameters lnh_m and σ were optimized for each soil sample j in MATLAB. The scaling approach, based on the similar media concept, identifies a representative pore-size distribution for the entire soil domain with the corresponding mean value of ln$h_{m,j}$ and a lognormal distribution of scaling factors, α_j (Nasta *et al.*, 2013). The scaling factors

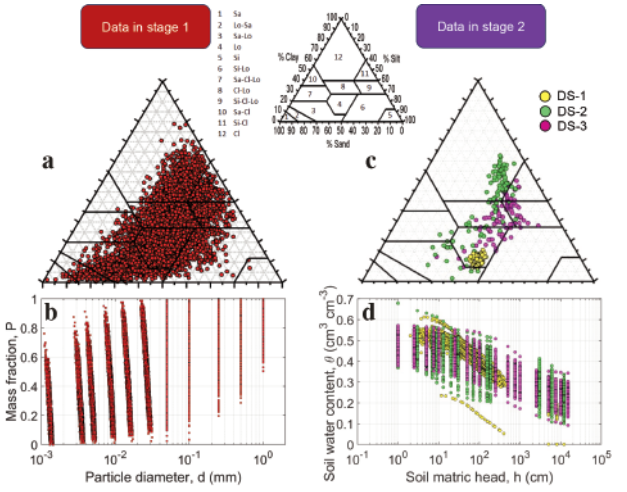

Figure 1. Data used in stage 1: **a**) textural distribution of the 4,128 soil samples collected in Campania (red circles); **b**) eleven particle-size distribution data relating particle diameter, d (mm) with corresponding particle mass fraction, P (red squares). Data used in stage 2: **c**) textural distribution of 89, 105, and 88 soil samples pertaining to DS-1 (yellow circles), DS-2 (green circles), and DS-3 (magenta circles), respectively; **d**) soil water retention data pairs measured on soil cores taken from DS-1 (yellow circles), DS-2 (green circles) and DS-3 (magenta circles), respectively.

Table 1. List of 27 particle-size distribution models with corresponding references and parameters. The number of input parameters is indicated by *p*.

Reference	Equation	Parameters	p
Millan *et al.* (2003)	$P(d) = a - exp\left[-\left(\frac{d}{b}\right)^{c}\right]$	a, *b*, *c*	3
Nemes *et al.* (1999)	$P(d) = a + b \times exp\{-exp[-c(d-D)]\}$	*a*, *b*, *c*, *D*	4
Nemes *et al.* (1999)	$P(d) = exp\{-exp[-c(d-D)]\}$	*c*, *D*	2
Zobeck *et al.* (1999)	$P(d) = \frac{1}{(a\times\sqrt{2\pi})\times\exp\left(-\frac{(-\log(d)-b)^2}{2\times a^2}\right)}$	*a*, *b*	2
Pasikatan *et al.* (1999)	$P(d) = normcdf\left(\frac{\ln(d-a)}{b}\right)$	*a*, *b* *normcdf*=normal cumulative distribution function in MATLAB	2
Buchan *et al.* (1989)	$P(d) = \frac{1}{2}\left\{1 + erf\left(\frac{lnd - \ln\bar{d}}{\sigma\sqrt{2}}\right)\right\} \quad lnd > \ln\bar{d}$ $P(d) = \frac{1}{2}\left\{1 - erf\left(\frac{lnd - \ln\bar{d}}{\sigma\sqrt{2}}\right)\right\} \quad lnd \le \ln\bar{d}$	$\ln\bar{d}, \sigma$	2
Buchan *et al.* (1993a)	$G(d) = (1-\varepsilon)\times P(d) + \varepsilon$	ε and P(*d*) is defined by SL model	3
Buchan *et al.* (1993b)	$G(d) = P(d) + c$	*c* and P(*d*) is defined by SL model	3
Kolev *et al.* (1996)	$P(d) = A\times\exp(B\times logd)$	*A*, *B*	2
Jaky (1944)	$P(d) = exp\left\{-\frac{1}{p^2}\left[ln\left(\frac{d}{d_{max}}\right)\right]^2\right\}$	*p* d_{max} is the largest diameter	1
Fredlund *et al.* (2000)	$P(d) = \left\{w\left[\frac{1}{\left[\ln\left[\exp(1)+\left(\frac{a}{d}\right)^n\right]\right]^m}\right] + (1 - w)\left[\frac{1}{\left[\ln\left[\exp(1)+\left(\frac{l}{d}\right)^k\right]\right]^l}\right]\right\} \times\left\{1 - \left(\frac{\ln(1+\frac{d_f}{d})}{\ln(1+\frac{d_f}{d_m})}\right)^7\right\}$	*a*, *n*, *m*, *w*, *j*, *k*, *l* d_m=0.0001 mm d_f=0.001 mm	7
Mandelbrot (1983)	$P(d > d_i) = Cd_i^{-D}$	*C*, *D*	2
Kravchenko & Zhang (1998)	$P(d) = exp\left\{lnk_2 + \left(\frac{3D^2-13D+14}{D^2-5D+4}+1\right)\times lnd\right\}$	k_2, *D*	2
Perrier (1999)	$P(d \le d_i) = k + d_i^{3-D}$	*k*, *D*	2
Bird *et al.* (2000)	$P(d \le d_i) = cd_i^{3-D}$	*c*, *D*	2
Perrier and Bird (2000)	$P(d \le d_i) = (a^{D-3})\times\left(\frac{d_i}{L}\right)^{3-D}$	*a*, *D* *L* is the largest particle size	2
Lassabatere *et al.* (2006)	$P(d) = \left[1 + \left(\frac{d_g}{d}\right)^n\right]^{-m}$; $m = 1 - \frac{2}{n}$	d_g, *n*	2
Haverkamp and Parlange (1986)	$P(d) = \left[1 + \left(\frac{k_1}{d}\right)^{k_2}\right]^{\frac{1}{k_2}-1}$	k_1, k_2	2
Schuhmann (1940)	$P(d) = \left[\frac{d}{d_{max}}\right]^a$	*a* d_{max} is the largest diameter	1
Nesbitt and Breytenbach (2006)	$P(d) = 10\left[\frac{1}{a+1}\times\left(\frac{d}{2}\right)^{a+1} + \left(0.1 - \frac{1}{a+1}\right)\times\left(\frac{d}{2}\right)^{\left(\frac{1}{\frac{1}{a+1}-0.1}\right)}\right]$	*a*	1
Pasikatan *et al.* (1999)	$P(d) = \left(\frac{k_1}{1-k_2}\right)\times d^{(1-k_2)}$	k_1, k_2	2
Harris (1968)	$P(d) = 1 - \left[1 - \left(\frac{d}{d_{max}}\right)\right]^a$	*a* d_{max} is the largest diameter	1
Zhuang *et al.* (2001)	$P(d) = a\times\ln(d) + b$	*a*, *b*	2
Rosin and Rammler (1933)	$P(d) = 1 - exp(-ad^b)$	*a*, *b*	2
Pasikatan *et al.* (1999)	$P(d) = \exp(-\beta_1\times d^{\beta_2})$	β_1, β_2	2
Andersson (1990)	$P(d) = a + b\,arctg\left[c\,ln\left(\frac{d}{e}\right)\right]$	*a*, *b*, *c*, *e*	4
Liu *et al.* (2004)	$P(d) = \frac{1}{1 + a\,exp(-bd^c)}$	*a*, *b*, *c*	3

Non-commercial use only

quantify the deviation of the $\ln h_{m,j}$ pertaining to different locations with respect to their mean value referred to a reference soil of the study area. The geometric scaling describes the spatial variability of soil hydraulic properties through the field standard deviation, namely σ^*, which is defined as the spatial-mean of σ_j.

In this study the soil water retention function was estimated from knowledge of the PSD, ρ_b, and θ_s using the following PTFs: the AH PTF (Arya and Heitman, 2015), and the MV PTF (Mohammadi and Vanclooster, 2011). The uniform-size fraction masses, ω_i (-) at particle size i, were obtained by using a PSD model. A total of eleven soil water content values, θ_i (cm^3 cm^{-3}), corresponding to ω_i, were obtained by using the following equation:

$$\theta_i = \theta_s \sum_{i=1}^{n} w_i; \quad i=1, 2, 3, \dots n \tag{6}$$

The PTF-AH estimates the soil matric pressure head, h_i for a given fraction of particles as:

$$h_i = \frac{0.149}{\sqrt{\frac{0.0717\varepsilon(w_i/\rho_b)}{n_i^{4/3} d_i/2}}} \tag{7}$$

where d_i (cm) is the particle diameter and n_i is the number of spherical particles for each i-th fraction while ε (cm^3 cm^{-3}) is soil porosity defined as 1-ρ_b/ρ_s, where ρ_s is the particle density assumed in this study as 2.65 g cm^{-3}.

The PTF-MV model estimates the soil matric pressure head, h_i for a given fraction of particles as:

$$h_i = \frac{0.00543}{d_i/2}\xi \tag{8}$$

where the particle diameter is expressed in m and needs to be converted into units of cm while ξ (dimensionless) is a packing coefficient expressed as:

$$\xi = \frac{1.9099}{1+e} \tag{9}$$

where e is the void ratio defined as:

$$e = \frac{\rho_s - \rho_b}{\rho_b} \tag{10}$$

The goodness of fit was assessed in terms of RMSR (Eq. 1) by using the decimal logarithmic transform of experimental and predicted matric pressure head values. The measure of prediction performance was computed in terms of integral mean deviation (IMD) and integral root mean square deviation (IRMSD) as follows:

$$IMD = \frac{1}{(\zeta_u - \zeta_l)} \int_{\zeta_l}^{\zeta_u} [\theta(\zeta)_{LAB} - \theta(\zeta)_{PTF}]\, d\zeta \tag{11}$$

and

$$IRMSD = \left\{ \frac{1}{(\zeta_u - \zeta_l)} \int_{\zeta_l}^{\zeta_u} [\theta(\zeta)_{LAB} - \theta(\zeta)_{PTF}]^2\, d\zeta \right\}^{1/2} \tag{12}$$

where $\xi = \log_{10}(|h|)$, $\theta(\xi)_{LAB}$ and $\theta(\xi)_{PTF}$ are the observed and predicted (either AH or MV) soil water content as a function of ξ. The water retention functions were integrated between the lower (ζ_l = 0) and upper (ζ_u = 4.2) limits. IMD and IRMSD are expressed in cm^3 cm^{-3}. The IMD reveals biases in prediction (meaning underprediction when IMD > 0 cm^3 cm^{-3}) while IRMSD indicates the dispersion of deviations. Optimal predictions would lead to IMD = 0 cm^3 cm^{-3} (perfect accuracy) and IRMSD = 0 cm^3 cm^{-3} (perfect precision).

The prediction performance was evaluated as a function of soil matric head by using the mean relative error (MRE) between observed and estimated soil water retention values, expressed as:

$$MRE(h)\% = \frac{1}{N}\sum_{i=1}^{N}\left[1 - \frac{\theta(h)_{PTF,i}}{\theta(h)_{LAB,i}}\right] \times 100 \tag{13}$$

where i is the counter and N is the total number of soil matric pressure heads. MRE is expressed here in percentage units (%) and should be 0% if the prediction was optimal.

Experimental data and MATLAB scripts are provided by the authors upon request.

Results

Evaluation of twenty-seven models to fit the particle-size distribution curve by using 4128 soil samples

Figure 2 shows the RMSR values of the twenty-seven PSD models fitted on the eleven PSD data of the 4128 soil samples. The best fit was obtained using the bimodal PSD model proposed by Fredlund *et al.* (2000) based on seven parameters with 25th and 75th percentiles equal to 0.0038 and 0.0083, respectively. The worst performance came from the Harris model based on the use of one fitting parameter with 25th and 75th percentiles equal to 0.1124 and 0.1604, respectively. Yet, the RMSR criterion does not account for parameter redundancy and a concomitant low number of PSD data. For this reason, we also computed AICc values, which are depicted in Figure 3.

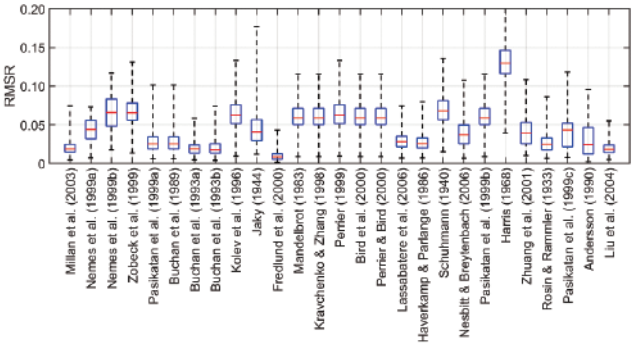

Figure 2. Boxplots of root mean square residual values for the 27 particle-size distribution models. On each box, the red horizontal line indicates the median, and the bottom and top edges of the box indicate the 25th and 75th percentiles, respectively. The whiskers (black dashed lines) extend to the most extreme data points not considered outliers.

Non-commercial use only

Parsimonious PSD models based on the use of two or three calibration parameters take on relatively low AICc values and show excellent performance. The statistical distributions of the performance indicators do not always follow a normal statistical distribution and, therefore, Table 2 lists the performance metrics in terms of median values (Rosin and Rammler, 1933; Schuhmann, 1940; Jaky, 1944; Harris, 1968; Mandelbrot, 1983; Buchan, 1989; Kolev *et al.*, 1996; Nemes *et al.*, 1999; Pasikitan, 1999; Zobeck *et al.*, 1999; Bird *et al.*, 2000; Zhuang *et al.*, 2001; Perrier and Bird, 2002; Nesbitt and Breytenbach, 2006). The PSD models were ranked according to the median RMSR values which dictated the prediction uncertainty.

A perusal of the median values of the performance metrics presented in Table 2 shows that no model has been able to satisfy the three metrics. The Fredlund *et al.* (2000) model has the best median value of RMSR and R^2_{adj}, but not the best AICc. On the other hand, the model developed by Buchan *et al.* (1993) has the best AICc median, and is closely followed by the models of Millan *et al.* (2003), Liu *et al.* (2014) and Buchan *et al.* (1993a).

The multi-parametric PSD models proposed by Andersson (1990) and Fredlund *et al.* (2000) were penalized for parameter redundancy (p=4 and p=7, respectively) against the paucity of

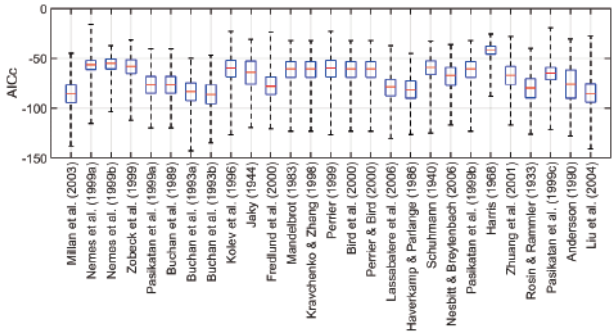

Figure 3. Boxplots of corrected Akaike information criterion values for the 27 particle-size distribution models. On each box, the red horizontal line indicates the median, and the bottom and top edges of the box indicate the 25th and 75th percentiles, respectively. The whiskers (black dashed lines) extend to the most extreme data points not considered outliers.

Table 2. Median values of the 4,128 root-mean-square residual, corrected Akaike information criterion, and adjusted coefficient of determination (R^2_{adj}). In this table, the 27 particle-size distribution models were ranked according to the median values of root-mean-square residual.

Reference	p	RMSR	AICc	R^2_{adj}
Fredlund *et al.* (2000)	7	0.0055	-78.16	0.998
Buchan *et al.* (1993b)	3	0.0134	-86.21	0.995
Millan *et al.* (2003)	3	0.0138	-85.60	0.995
Liu *et al.* (2004)	3	0.0140	-85.31	0.995
Buchan *et al.* (1993a)	3	0.0153	-83.24	0.994
Andersson (1990)	4	0.0175	-75.95	0.991
Haverkamp and Parlange (1986)	2	0.0196	-81.34	0.992
Rosin and Rammler (1933)	2	0.0211	-79.71	0.990
Lassabatere *et al.* (2006)	2	0.0219	-78.89	0.989
Pasikatan *et al.* (1999)	2	0.0246	-76.32	0.987
Buchan *et al.* (1989)	2	0.0246	-76.32	0.987
Zhuang *et al.* (2001)	2	0.0373	-67.18	0.970
Pasikatan *et al.* (1999)	2	0.0414	-64.84	0.963
Nesbitt and Breytenbach (2006)	1	0.0422	-67.26	0.964
Nemes *et al.* (1999)	4	0.0430	-56.24	0.942
Jaky (1944)	1	0.0487	-64.12	0.952
Mandelbrot (1983)	2	0.0499	-60.75	0.943
Kravchenko & Zhang (1998)	2	0.0499	-60.75	0.943
Bird *et al.* (2000)	2	0.0499	-60.75	0.943
Perrier and Bird (2000)	2	0.0499	-60.75	0.943
Pasikatan *et al.* (1999)	2	0.0499	-60.75	0.943
Perrier (1999)	2	0.0521	-59.78	0.936
Kolev *et al.* (1996)	2	0.0522	-59.78	0.936
Zobeck *et al.* (1999)	2	0.0569	-57.87	0.926
Schuhmann (1940)	1	0.0608	-59.25	0.925
Nemes *et al.* (1999)	2	0.0650	-54.95	0.907
Harris (1968)	1	0.1370	-41.37	0.628

AICc, Akaike information criterion; RMSR, root-mean-square residual; R^2a_{dj}, adjusted coefficient of determination.

Non-commercial use only

experimental PSD data (n=11). The contour maps of RMSR values in the USDA textural triangle indicate variable performance for the parsimonious PSD models of Buchan *et al.* (1993b) and Millan *et al.* (2003) (Figure 4a-b). The prediction performance becomes worse for the loamy-sand and sandy-clay-loam classes, whereas low RMSR values are observed in the cases of clay, clay-loam, and loam textural classes. By contrast, the RMSR values obtained from the Fredlund *et al.* (2000) model are excellent in almost all soil textural classes (Figure 4c).

Evaluation of shape similarity between particle-size distribution and water retention function

Based on the outcome of the previous analysis, we selected as optimal PSD models those developed by Buchan *et al.* (1993b), Fredlund *et al.* (2000), and Millan *et al.* (2003). These three PSD models were combined with PTF-AH and PTF-MV to evaluate the potential of these two PTFs in providing estimates of the WRF.

Figure 5 shows the cumulative distributions of RMSR when using the data taken from the DS-1 and DS-2 datasets. The degree of spatial variability of soil properties, as expressed by the value of σ^*, was obtained from the scaling approach (depicted by the vertical dashed line in Figure 5). In the most uniform site (DS-1), the RMSR medians of 0.51, 0.58, and 1.03 were obtained when combining the PTF-AH with the PSD models of Fredlund *et al*. (2000), Buchan *et al*. (1993b) and Millan *et al*. (2003), respectively. The PTF-AH outperformed the PTF-MV, which obtained RMSR values between 0.92 and 1.10. Both PTFs provided reasonable performance within the acceptance threshold (RMSR<σ^*). By contrast, in the case of the second field (DS-2) with high spatial variability of soil properties, the PTF-MV (3% to 6% RMSR>σ^*) outperformed the PTF-AH (8% to 30% RMSR>σ^*). The RMSR medians ranged between 2.30 (Fredlund *et al*., 2000) and 3.66 (Millan *et al*., 2003) when using the PTF-AH, and between 1.46 (Fredlund *et al*., 2000) and 2.05 (Millan *et al*., 2003) when using the PTF-MV. However, the majority of RMSR median values were larger than those obtained in the original studies of Arya and Heitman (2015) and Mohammadi and Vanclooster (2011). The 89 soil samples in DS-1 (Acerra dataset) were collected along a 132-m-long transect in a peach orchard located near the city of Acerra. The loamy soil was a typical volcanic Andosol and fairly uniform. By contrast, DS-2 (Alento dataset) comprised a total of 105 soil samples that were collected along six different transects distributed over the Upper Alento River Catchment (an upland area of approximately 100 km^2). The dominant soil texture classes were clay and clay-loam. Indeed, the σ^* in DS-2 doubles if compared to that obtained for DS-1. As expected, the predictive performance in DS-2 worsens significantly, especially when applying the PTF-AH. For the sake of brevity, the results of DS-3 (Fiumarella dataset) are not shown. The RMSR median values for the PTF-AH range between 1.63 and 2.43 and for PTF-MV range between 1.48 and 1.78. The vast majority of RMSR values are lower than the acceptance threshold (σ^*=4.25) when the WRF is estimated by using the PTF-MV. In general, the use of the PSD model proposed by Fredlund *et al*. (2000) ensures very good performances when using both PTFs for all datasets. The parsimonious PSD model proposed by Buchan *et al*. (1993b) provides a similar performance in DS-1 but lower performance in DS-2 and DS-3 than that provided by Fredlund *et al*. (2000). The combination of the optimal three PSD models (Buchan *et al.*, 1993b; Millan *et al.*, 2003; Fredlund *et al.*, 2000) with the PTF-AH (red lines) and the PTF-MV (green lines) was also evaluated with regard of a wider range of h-values in the water retention function, namely from near saturation to extremely dry soil conditions (wilting point). We selected a range of soil matric suction head, $|h|$ (*i.e.*, the absolute value of h) from 0.1 cm (=10^{-1} cm) to 15,296 cm (=$10^{4.2}$ cm). The values of mean relative error, MRE (%), between the measured and estimated soil water retention values were depicted in Figure 6 and revealed the magnitude of bias as a function of $|h|$. Obviously, the use of the measured saturated soil water content in both PTFs led to unbiased predictions near saturation, whereas a discrepancy between observed and predicted soil water contents becomes

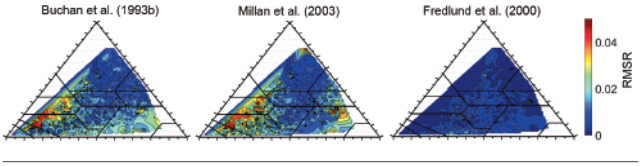

Figure 4. Contour maps of root mean square residual obtained by using the particle-size distribution models proposed by Buchan *et al.* (1993b), Millan *et al.* (2003), and Fredlund *et al.* (2000).

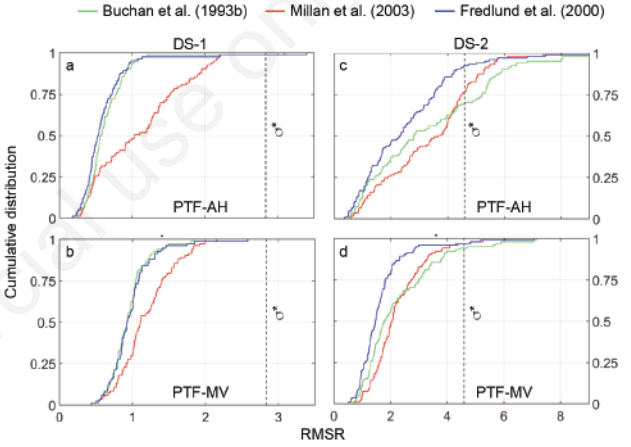

Figure 5. Cumulative distributions of root-mean-square residual between experimental and predicted log transforms of soil matric pressure heads for the selected three particle-size distribution models (Buchan *et al.,* 1993b; Millan *et al.*, 2003; Fredlund *et al.*, 2000). These particle-size distribution models were implemented **a**) in PTF-AH; **b**) in PTF-MV when using the 89 soil samples in DS-1 (Acerra dataset); **c**) in PTF-AH; **d**) in PTF-MV when using the 105 soil samples in DS-2 (Alento dataset). The vertical dashed line indicates the acceptance threshold, σ* computed by using the scaling results on the measured water retention functions.

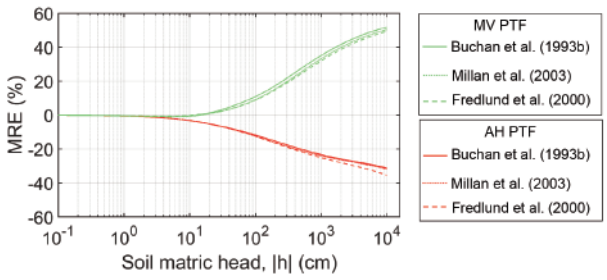

Figure 6. Mean relative error (%) as a function of soil matric suction head, |h| (cm) when using PTF-AH (red lines) and PTF-MV (green lines) combined to Buchan *et al.* (1993b) (solid line), Millan *et al.* (2003) (dotted line), Fredlund *et al*. (2000) (dashed line).

Non-commercial use only

OPEN ACCESS

increasingly evident when approaching drier soil conditions. As the curves in Figure 6 clearly show, it is interesting to note that the two tested PTFs have a different behavior. PTF-AH (red line) overestimates the measured WRF as indicated by negative MRE values. The worst MRE value of -35.4% at the wilting point was obtained by using the Fredlund *et al.* (2003) PSD model (dashed red line). Instead, systematic underpredictions of the measured WRF were obtained when using PTF-MV (green line) by reaching the slightly worse MRE value of +51.7% at the wilting point when this PTF is combined with Buchan *et al.* (1993b) PSD model (solid green line).

Figure 7 displays the IMD (cm^3 cm^{-3}) and IRMSD (cm^3 cm^{-3}) of the parsimonious PSD model of Buchan *et al.* (1993b) when combined with both PTF-AH and PTF-MV. These two PTFs show prediction biases at different textural classes. Near-zero (accurate) and negative (indicating overestimation of the WRF) IMD values in the loam (green color) and in the clay and silt-clay (bluish color) texture classes, respectively, were obtained when using the PTF-AH (Figure 7a). By contrast, negative (indicating underestimation) IMD values were obtained in the loam and clay-loam classes when using the PTF-MV. However, PTF-MV suffers from overestimation as does PTF-AH for fine-textured soils (Figure 7b). The precision indicated by the IRMSD values reflected different patterns in the soil textural triangle when using the two PTFs (Figure 7c and 7d). In general, accuracy and precision are excellent only in a few spots and fair for most textural classes of the USDA triangle. Cornelis *et al.* (2001) recommend using the integral Pearson correlation coefficient in addition to IMD and IRSDM to optimally rank different PTFs. In this study, we evaluated only two PTFs to assess the hypothesis of shape similarity between PSD and WRF.

Discussion

The PSD data used in this study have been all measured using the same method, namely the hydrometer method combined with the sieving method. This technique is quite a standard in almost all the soil laboratories around the world, even though it requires skilled operators and is subject to measurement errors that can occur primarily when inserting the hydrometer into the suspension. Nevertheless, the experimental protocol used in this study ensures virtually similar measurement uncertainty and equitable comparisons (the same number of measurement steps for each soil sample) among the 4,128 soil samples.

The AICc and R^2_{adj} performance metrics indicated that the parsimonious PSD models based on 2-3 parameters are recommended to fit the eleven experimental PSD data. AICc penalizes the Fredlund *et al.* (2000) PSD model for parameter redundancy and concurrent experimental data paucity. Therefore, more experimental efforts are required to increase the number of measurements to fit the flexible model proposed by Fredlund *et al*. (2000) which provides a uni- or multi-modal shape of the PSD.

The analyses conducted in this study are of practical use to quantify the uncertainty associated with PSD models employed to predict the soil WRF through PTFs based on the concept of shape similarity between PSD and pore-size distribution (Arya and Paris, 1981; Haverkamp and Parlange, 1986; Arya *et al.*, 1999; Haverkamp *et al.*, 2002; Chan and Govindaraju, 2004; Hwang and Choi, 2006; Arya *et al.*, 2008; Mohammadi and Meskini-Vishkaee, 2013; Mohammadi and Vanclooster, 2011). For example, the BEST algorithm implemented in the Beerkan method estimates van Genuchten's water retention shape parameters (van Genuchten, 1980) from the shape parameters fitted on the PSD (Lassabatere *et al.*, 2006). The Buchan PSD model was used by Nasta *et al.* (2013) to exploit its similarity to the Kosugi analytical relation describing the WRF (Kosugi, 1996).

Both physico-empirical PTF-AH and PTF-MV do not need calibration using training data sets. For this reason, these PTFs remove the dependency on experimental data and can be assumed as universally valid.

The direct measurement of oven-dry soil bulk density and saturated water content ensures the arrangement of solid particles in the natural state of packing and optimal prediction of WRF near saturation when using the physico-empirical PTFs. To reduce the efforts required in intensive field campaigns and tedious laboratory experiments, one can rely on the PTF developed in Campania by Palladino *et al.* (2022) to estimate oven-dry soil bulk density (ρ_b) and saturated water content (θ_s) by using textural classes (sand, silt, and clay contents) and soil organic content (OC). Figure 8 shows the impact of using measured or estimated ρ_b data when combining the Buchan *et al.* (1993b) PSD model with PTF-AH and PTF-MV on 105 data pertaining to DS-2 (Alento dataset). The direct measurement of ρ_b and θ_s provides median RMSR values of 2.81 and 1.78 for PTF-AH and PTF-MV, respectively. In contrast, the use of the PTF developed by Palladino *et al.* (2022) deteriorates model performance by reducing the spatial variability of WRF near saturation. Indeed, the information on soil texture and organic content is unable to reproduce the spatial variability of the measured soil bulk density. Nevertheless, the PTF-AH and PTF-MV obtained RMSRs of 4.28 and 2.94, respectively, which are still lower than the acceptance threshold (σ^*=4.59).

The causes of the bias in predicting the WRF from texture measurements are primarily due to a violation of assuming the existence of a shape similarity between PSD and WRF for some soil samples as well as the unavoidable limitations of a simplified estimation technique such like a PTF. On the one hand, Mohammadi (2018) disputed the expression for pore radii (Eq. 3 in Arya and Heitman, 2015), which might have generated the systematic overestimation of WRF observed in our analysis. Arya and

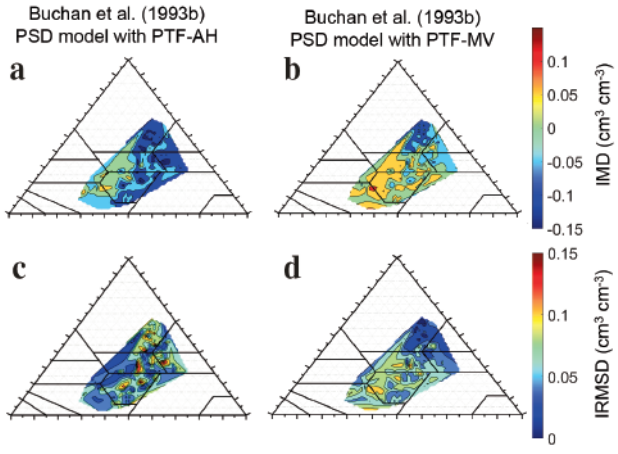

Figure 7. Contour maps of integral mean deviation, integral mean deviation (cm^3 cm^{-3}) obtained by using the particle-size distribution models proposed by Buchan *et al.* (1993b) combined to **a**) PTF-AH; **b**) PTF-MV and integral root mean square deviation, integral root mean square deviation (cm^3 cm^{-3}) obtained by using the particle-size distribution models proposed by Buchan *et al.* (1993b) combined to **c**) PTF-AH, **d**) PTF-MV.

Non-commercial use only

Heitman supported their approach that, however, needs to be further verified using additional independent datasets (Arya and Heitman, 2018). The PTF-MV outperformed the PTF-AH in northwestern China by using 170 soil samples distributed over eight texture classes (Li *et al*., 2016). The PTF-AH systematically overestimated the observed WRFs while PTF-MV slightly underestimated and overestimated the observed soil water content values in the dry and wet region of the WRF, respectively (Li *et al*., 2016). The underestimation of soil water content values in the dry region of the retention function can be definitely attributed to the existence of water films absorbed by the solid particles, a situation that is overlooked in the PTF-MV (Tuller and Or, 2001). Shang and Li (2019) report an underestimation of the observed water content values in the dry region when predicting the WRF with PTF-MV in northwest China. Meskini-Vishkaee *et al.* (2014) proposed a physically-based scaling approach to reduce the underestimation of WRF in the dry region when using the PTF-MV (Chang *et al.*, 2019). This scaling approach might potentially enhance model performance by 30% as stated by Meskini-Vishkaee *et al.* (2014).

Another potential drawback might arise from the use and misuse of the residual water content (θ_r) parameter, as questioned by Chang *et al.* (2019). However, in this study, we always assumed θ_r=0 cm^3 cm^{-3} to reduce uncertainty and subjectivity when fitting the water retention curve on measured soil water content and matric head data pairs, and when converting the particle mass fraction into soil water content both PTFs (Eq. 6).

The presence of macropores is mainly related to soil structure rather than to the primary soil particles that identify the textural class of a soil (Shang and Li, 2019). The use of a bimodal or multimodal water retention function ensures a proper description of the pore-size distribution which is given by the aggregation of the primary particles into secondary and tertiary particles (Li *et al.*, 2014; Haghverdi 2020; Hassan *et al.* 2022; Zhang *et al.*, 2022). The flexibility of PSD models based on a large number of parameters (Fredlund *et al*., 2000) enhance the prediction performance of the two physico-empirical PTFs analyzed in this study. To do so, the number of PSD measurements needs to be incremented to ensure a reliable fit. This would be beneficial for predicting the hydraulic conductivity function from knowledge of the WRF described by a bimodal shape (Romano *et al.*, 2011; Romano and Nasta, 2016).

Conclusions

To the best of our knowledge, only a few physico-empirical PTFs based on the hypothesis of shape similarity between PSD and WRF exist in the literature. In this study, the prediction capability of two PTFs (PTF-AH and PTF-MV) was evaluated using 282 soil samples gathered in the regions of Campania and Basilicata in southern Italy. In a preliminary stage, the accuracy of PSD twenty-seven PSD models for fitting texture measurements was evaluated and we selected the best three PSD models. The best parsimonious model was the equation proposed by Buchan *et al.* (1993b).

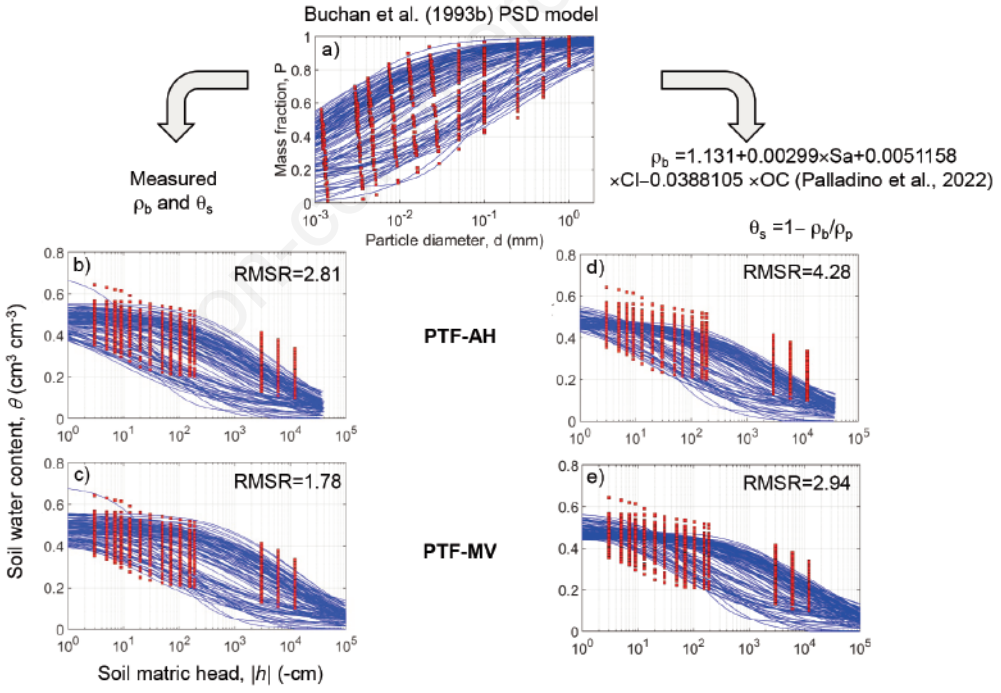

Figure 8. Use of PTF-AH and PTF-MV to estimate the water retention function by using particle-size distribution, soil bulk density (ρ_b), organic carbon content, and saturated water content (θ_s) in DS-2 (Alento dataset) with the following procedure: **a**) fit of the Buchan *et al.* (1993b) particle-size distribution model (blue line) on measured particle-size distribution data (red squares); comparison between measured (red squares) and estimated (blue line) water retention functions when applying **b**) PTF-AH and **c**) PTF-MV with measured ρ_b, and θ_s and **d**) PTF-AH and **e**) PTF-MV with ρb predicted with the pedotransfer functions proposed by Palladino *et al.* (2022) where θ_s is assumed equal to soil porosity and soil particle density is fixed at 2.65 g cm^{-3}. Sa (%) and Cl (%) indicate sand and clay contents, respectively. The root mean square residual between experimental and predicted log transforms of soil matric pressure head values are reported as performance metrics for both PTF-AH and PTF-MV.

The study presented in this paper verified the applicability of two physico-empirical PTFs to estimate the water retention function from knowledge of particle-size distribution, oven-dry bulk density, and saturated water content. The PTF-AH and PTF-MV are calibration-free models and for this reason, these PTFs are attractive for practical applications at regional scale. The hypothesis of shape similarity was accepted when the prediction precision was lower than the spatial variability of the measured soil hydraulic properties, which was quantified through the similar media concept developed by Kosugi *et al.* (1998). In general, the majority of the tested PSD models led to a reasonable performance by sustaining the hypothesis of shape similarity. Both physico-empirical PTFs provided from excellent to fair performance in estimating the 282 WRFs and we have also raised critical explanations for the model flaws. The use of PTF-AH and PTF-MV might substantially reduce excessive experimental efforts, especially if the oven-dry bulk density and saturated water content are predicted by using *ad-hoc* empirical region-specific PTFs based on knowledge of soil texture and soil organic carbon content.

Finally, it may be worth noting that the best PSD models (Buchan *et al.*, 1993b; Millan *et al.*, 2003; Fredlund *et al.*, 2000) selected in Campania provided reasonable performance when combined with the PTF-AH and PTF-MV even for the soils of the third test area (DS-3) belonging to the Basilicata region. This outcome deserves further investigation which will be presented in a subsequent paper.

References

Allocca C., Castrignanò A., Nasta P., Romano N. 2023. Regional-scale assessment of soil functions and resilience indicators: Accounting for change of support to estimate primary soil properties and their uncertainty. Geoderma 431:116339,

Andersson S. 1990. Markfysikaliska undersökningar i odlad jord,XXVI. Om mineraljordens och mullens rumsutfyllande egenskaper. En teoretisk studie. (In Swedish). Swedish University of Agricultural Sciences, Uppsala, p. 70.

Antinoro C., Bagarello V., Ferro V., Giordano G., Iovino M. 2014. A simplified approach to estimate water retention for Sicilian soils by the Arya–Paris model. Geoderma 213:226-34.

Arya L.M., Paris J.F. 1981. A physico-empirical model to predict the soil moisture characteristic from particle-size distribution and bulk density data. Soil Sci. Soc. Am. J. 45:1023-30.

Arya L.M., Heitman J.L. 2015. A non-empirical method for computing pore radii and soil water characteristics from particle-size distribution. Soil Sci. Soc. Am. J. 79:1537-44.

Arya L.M., Bowman D.C., Thapa B.B., Kassel D.K. 2008. Scaling soil water characteristics of golf course and athletic field sands from particle-size distribution. Soil Sci. Soc. Am. J. 72:25-32.

Arya L.M., Leij F.J., van Genuchten Mth., Shouse P. 1999. Scaling parameter to predict the soil water characteristic from particle-size distribution data. Soil Sci. Soc. Am. J. 63:510-9.

Arya L.M., Heitman J.L. 2018. Response to "Comment on 'A Non-Empirical Method for Computing Pore Radii and Soil Water Characteristics from Particle Size Distribution' by Arya and Heitman (2015)" Soil Sci. Soc. Am. J. 82:1595-6.

Ayoubi S., Karami M. 2019. Pedotransfer functions for predicting heavy metals in natural soils using magnetic measures and soil properties. J. Geochem. Explor. 197:212-9.

Bah A.R., Kravchuk O., Kirchhof G. 2009. Fitting performance of particle-size distribution models on data derived by conventional and laser diffraction techniques. Soil Sci. Soc. Am. J. 73:1101-7.

Bayat H., Rastgo M., Zadeh M.M., Vereecken H. 2015. Particle size distribution models, their characteristics and fitting capability. J. Hydrol. 529:872-89.

Bayat H., Rastgou M., Nemes A., Mansourizadeh M., Zamani P. 2017. Mathematical models for soil particle-size distribution and their overall and fraction-wise fitting to measurements. Eur. J. Soil Sci. 68:345-64.

Bird N., Perrier E., Rieu M. 2000. The water retention function for a model of soil structure with pore and solid fractal distributions. Eur. J. Soil Sci. 51:55-63.

Bittelli M., Flury M. 2009. Errors in water retention curves determined with pressure plates. Soil Sci. Soc. Am. J. 73:1453-60.

Bouyoucos G.J. 1951. A recalibration of the hydrometer method for making mechanical analysis of soils. Agron. J. 43:434-8.

Buchan G.D. 1989. Applicability of the simple lognormal model to particle-size distribution in soils. Soil Science. 147:155-61.

Buchan G.D., Grewal K., Robson A. 1993. Improved models of particle-size distribution: an illustration of model comparison techniques. Soil Sci. Soc. Ame. J. 57:901-8.

Campos-Guereta I., Dawson A., Thom N. 2021. An alternative continuous form of Arya and Paris model to predict the soil water retention curve of a soil. Adv. Water Res. 154:103968.

Chan T.P., Govindaraju R.S. 2004. Estimating soil water retention curve from particle-size distribution data based on polydisperse sphere systems. Vadose Zone J. 3:1443-54.

Chang C.C., Cheng D.H., Qiao X.Y. 2019. Improving estimation of pore size distribution to predict the soil water retention curve from its particle size distribution. Geoderma 340:206-212.

Cheshmberah F., Zolfaghari A.A., Taghizadeh-Mehrjardi R., Scholten T. 2022. Evaluation of mathematical models for predicting particle size distribution using digital soil mapping in semiarid agricultural lands. Geocarto Int. 37:1-23.

Ciollaro G., Romano N. 1995. Spatial variability of the hydraulic properties of a volcanic soil. Geoderma 65:263-82.

Cornelis W.M., Ronsyn J., Van Meirvenne M., Hartmann R. 2001. Evaluation of pedotransfer functions for predicting the soil moisture retention curve. Soil Sci. Soc. Am. J. 65:638-48.

Esmaeelad L., Siavashi F., Seyedmohammadi J., Shabanpour M. 2016. The best mathematical models describing particle size distribution of soils. Model. Earth Syst. Environ. 2:166.

Fredlund M.D., Fredlund D., Wilson G.W. 2000. An equation to represent grain-size distribution. Can. Geotech. J. 37:817-27.

Gee G.W., Bauder J.W. 1986. Particle-size analysis. In: Klute, A. (Ed.), Methods of Soil Analysis. Part 1, 2nd ed. Agron. Monogr. 9. ASA and SSSA, Madison, WI, pp. 383-411.

Gee G.W., Or D. 2002. Particle-size analysis. In: Dane, J.H., Topp, G.C. (Eds.), Methods of Soil Analysis: Part 4 – Physical Methods. SSSA Book Series 5, Madison, USA, pp. 255-93.

Haghverdi A., Öztürk H.S., Durner W. 2020. Studying unimodal, bimodal, PDI and bimodal-PDI variants of multiple soil water retention models: II. Evaluation of parametric pedotransfer functions against direct fits. Water. 12:896.

Harris C. 1968. The application of size distribution equations to multi-event comminution processes. Transactions of the Institution of Mining Metallurgy, London, 241:343-58.

Hassan S.B.M., Dragonetti G., Comegna A., Sengouga A., Lamaddalena N., Coppola A. 2022. A bimodal extension of the ARYA & PARIS approach for predicting hydraulic properties of structured soils. J. Hydrol. 610:127980.

Haverkamp R., Parlange J.-Y. 1986. Predicting the water-retention

curve from particle-size distribution: 1. Sandy soils without organic matter. Soil Sci. 142:325-39.
Haverkamp R., Reggiani P., Nimmo J.R. 2002. Property-Transfer Models. pp. 759-82. In J.H. Dane and G.C. Topp (ed.) Methods of soil analysis. Part 4. SSSA Book Series No. 5. SSSA, Madison, WI.
Hwang S.I. 2004. Effect of texture on the performance of soil particle-size distribution models. Geoderma. 123:363-71.
Hwang S.I., Lee K.P., Lee D.S., Powers S.E. 2002. Models for estimating soil particle-size distributions. Soil Sci. Soc. Ame. J. 66:1143-50.
Hwang S.I., Choi S.I. 2006. Use of a lognormal distribution model for estimating soil water retention curves from particle-size distribution data. J. Hydrol. 323:325-34.
Jaky J. 1944. Soil Mechanics. Egyetemi Nyomda, Budapest (in Hungarian).
Kolev B., Rousseva S., Dimitrov D. 1996. Derivation of soil water capacity parameters from standard soil texture information for Bulgarian soils. Ecol. Modell. 84:315-9.
Kosugi K. 1996. Log-Normal distribution model for unsaturated soil hydraulic properties. Water Resour. Res. 32:2697-703.
Kosugi et al, 1998
Lassabatere L., Angulo-Jaramillo R., Soria Ugalde J., Cuenca R., Braud I., Haverkamp R. 2006. Beerkan estimation of soil transfer parameters through infiltration experiments – BEST. Soil Sci. Soc. Ame. J. 70:521-32.
Lee T.-K., Ro H.-M. 2014. Estimating soil water retention function from its particle-size distribution. Geosci. J. 18:219-30.
Li X., Li J.H., Zhang L.M. 2014. Predicting bimodal soil–water characteristic curves and permeability functions using physically based parameters. Comput. Geotech. 57:85-96.
Li D., Gao G., Shao M., Fu B. 2016. Predicting available water of soil from particle-size distribution and bulk density in an oasis-desert transect in northwestern China. J. Hydrol. 538:539-50.
Mandelbrot B.B. 1983. The Fractal Geometry of Nature. Macmillan, Freeman, San Francisco, CA.
Mebius L.J. 1960. A rapid method for the determination of organic carbon in soil. Anal. Chim. Acta. 22:120-4.
Meskini-Vishkaee F., Mohammadi M.H., Vanclooster M. 2014. Predicting the soil moisture retention curve, from soil particle size distribution and bulk density data using a packing density scaling factor. Hydrol. Earth Syst. Sci. 18:4053-63.
Meskini-Vishkaee F., Davatgar N. 2018. Evaluation of di□erent predictor models for detailed soil particle-size distribution. Pedosphere. 28:157-64.
Millan H., Gonzalez-Posada M., Aguilar M., Domınguez J., Cespedes L. 2003. On the fractal scaling of soil data. Particle-size distributions. Geoderma. 117:117-28.
Mohammadi M.H., Meskini-Vishkaee F. 2013. Predicting soil moisture characteristic curves from continuous particle-size distribution data. Pedosphere 23:70-80.
Mohammadi M.H. 2018. Comment on "A Non-Empirical Method for Computing Pore Radii and Soil Water Characteristics from Particle Size Distribution by Arya and Heitman (2015)." Soil Sci. Soc. Am. J. 82.
Mohammadi M.H., Vanclooster M. 2011. Predicting the soil moisture characteristic curve from particle size distribution with a simple conceptual model. Vadose Zone J. 10:594-602.
Nasta P., Kamai T., Chirico G.B., Hopmans J.W., Romano N. 2009. Scaling soil water retention functions using particle-size distribution. J. Hydrol. 374:223-34.
Nasta P., Romano N., Assouline S., Vrugt J.A., Hopmans J.W. 2013. Prediction of spatially-variable unsaturated hydraulic conductivity using scaled particle-size distribution functions. Water Resour Res. 49.
Nasta P., Szabó B., Romano N. 2021. Evaluation of Pedotransfer Functions for predicting soil hydraulic properties: A voyage from regional to field scales across Europe. J. Hydrol. Reg. Stud. 37.
Nemes A., Wösten J., Lilly A., Oude Voshaar J. 1999. Evaluation of different procedures to interpolate particle-size distributions to achieve compatibility within soil databases. Geoderma. 90:187-202.
Nesbitt A., Breytenbach W. 2006. A particle size distribution model for manufactured particulate solids of narrow and intermediate size ranges. Powder Technol. 164:117-23.
Nimmo J.R., Herkelrath W.N., Laguna Luna A.M. 2007. Physically based estimation of soil water retention from textural data: General framework, new models, and streamlined existing models. Vadose Zone J. 6:766-73.
Palladino M., Romano N., Pasolli E., Nasta P. 2022. Developing pedotransfer functions for predicting soil bulk density in Campania Region. Geoderma. 412:115726.
Pasikatan M., Steele J., Milliken G., Spillman C., Haque E. 1999. Particle size distribution and sieving characteristics of first-break ground wheat. Ame. Soc. Agric. Eng. 319:1-11.
Perrier E., Bird N. 2002. Modelling soil fragmentation: the pore solid fractal approach. Soil Tillage Res. 64:91-9.
Romano N., Santini A. 1999. Determining soil hydraulic functions from evaporation experiments by a parameter estimation approach: Experimental verifications and numerical studies. Water Resour. Res. 35:3343-59.
Romano N., Nasta P. 2016. How effective is bimodal soil hydraulic characterization? Functional evaluations for predictions of soil water balance. Eur. J. Soil Sci. 67:523-35.
Romano N., Hopmans J.W., Dane J.H. 2002. Water retention and storage: Suction table. In "Methods of Soil Analysis, Part 4, Physical Methods" (Dane J.H., and Topp G.C., eds.), SSSA Book Series N.5, Madison, WI, USA, 692-8 pp.
Romano N., Nasta P., Severino G., Hopmans J.W. 2011. Using bimodal log-normal functions to describe the hydraulic properties of soils. Soil Sci. Soc. Ame. J. 75:468-80.
Romano N., Nasta P., Bogena H.R., De Vita P., Stellato L., Vereecken H. 2018. Monitoring hydrological processes for land and water resources management in a Mediterranean ecosystem: the Alento River catchment observatory. Vadose Zone J. 17:180042.
Rosin P., Rammler E. 1933. The laws governing the fineness of powdered coal. J. Inst. Fuel. 7:29-36.
Russel J.C., Engle E.B. 1928. The organic matter content and color of soils in the central grassland states. In: Proceedings and Papers of the First International Congress of Soil Science (Deemer R.B., ed.), June 13-22, 1927, Washington, DC, USA.
Shang L., Li D. 2019. Comparison of di□erent approaches for estimating soil water characteristic curves from saturation to oven dryness. J. Hydrol. 577:123971.
Schuhmann J.R. 1940. Principles of comminution, I-size distribution and surface calculations. Min. Technol. 4:l-11.
Stokes G.G. 1850. On the effect of the internal friction of fluids on the motion of pendulums. Trans. Cambridge Philos. Soc. 9:8-106.
Tuller M., Or D. 2001. Hydraulic conductivity of variably saturated porous media: film and corner flow in angular pore space. Water Resour. Res. 37:1257-76.
van Genuchten M.Th. 1980. A closed form equation for predicting the hydraulic conductivity of unsaturated soils. Soil Sci. Soc.

Non-commercial use only

Am. J. 44:892-8.
Van Looy K., Bouma J., Herbst M., Koestel J., Minasny B., Mishra U., Montzka C., Nemes A., Pachepsky Y.A., Padarian J., Schaap M.G., Tóth B., Verhoef A., Vanderborght J., van der Ploeg M.J., Weihermüller L., Zacharias S., Zhang Y., Vereecken H. 2017. Pedotransfer functions in Earth system science: Challenges and perspectives. Rev. Geophys. 55:1199-256.
Vaz C.M.P., Ferreira E.J., Posadas A.D. 2020. Evaluation of models for fitting soil particle-size distribution using UNSODA and a Brazilian dataset. Geoderma Reg. 21:e00273.
Zhang Y., Weihermüller L., Tóth B., Noman M., Vereecken H. 2022. Analyzing dual porosity in soil hydraulic properties using soil databases for pedotransfer function development. Vadose Zone J. 21: e20227.
Zhuang J., Jin Y., Miyazaki T. 2001. Estimating water retention characteristic from soil particle-size distribution using a non-similar media concept. Soil Sci. 166:308-21.
Zobeck T.M., Gill T.E., Popham T.W. 1999. A two-parameter Weibull function to describe airborne dust particle size distributions. Earth Surf. Process. Landf. 24:943-55.
You T., Li S., Guo Y., Wang C., Liu X., Zhao J., Wang D. 2022. A superior soil–water characteristic curve for correcting the Arya-Paris model based on particle size distribution. J. Hydrol. 613:128393.

Non-commercial use only